Electronic Supplementary Material (ESI) for Metallomics

Leaf metallome preserved for 50 million years – Electronic Supplementary Information

N. P. Edwards[1], P. L. Manning*[1], U. Bergmann[2], P. L. Larson[3], B. E. van Dongen[1], W.I. Sellers[4], S. M. Webb[5], D. Sokaras[5], R. Alonso-Mori[5], K. Ignatyev[6], H. E. Barden[1], A. van Veelen[1], J. Anné[1], V. M. Egerton[1], R. A. Wogelius*[1]

[1]University of Manchester, School of Earth, Atmospheric, and Environmental Sciences, Williamson Research Centre for Molecular Environmental Science, M13 9PL, UK
[2]SLAC National Accelerator Laboratory, Linac Coherent Light Source, Menlo Park, CA, 94025, USA
[3]Black Hills Institute of Geological Research, Inc., Hill City, SD, 57745, USA
[4]University of Manchester, Faculty of Life Sciences, Manchester M13 9PL, UK
[5]SLAC National Accelerator Laboratory, Stanford Synchrotron Radiation Lightsource, Menlo Park, CA 94025, USA
[6]Diamond Light Source, Didcot, OX11 0DE, UK

S1 – Specimen Details

S1.1. Extant *Liquidambar styraciflua*

Identified by Leander Wolstenholme (Curator of Botany, Manchester Museum, pers. comm). Leaves of this species were collected directly from trees of Liquidambar styraciflua located on the grounds of the SLAC National Accelerator Laboratory in December 2009. Samples were immediately scanned by SRS-XRF at SSRL beamline 6-2. Boxes show approximate are of maps.

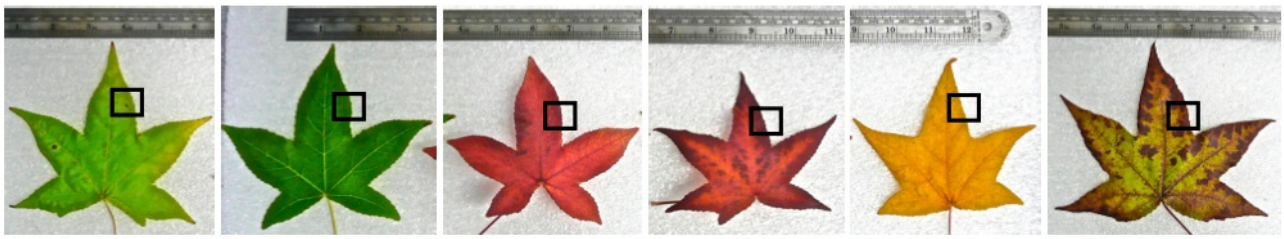

S1.2. Extant *Acer pseudoplatanus*

Leaves of this species were collected from labeled trees at the Jodrell Bank arboretum near Manchester, UK in May 2013 and analysed at Diamond Light Source (DLS) within a week of collection. Box shows approximate area of map obtained at DLS.

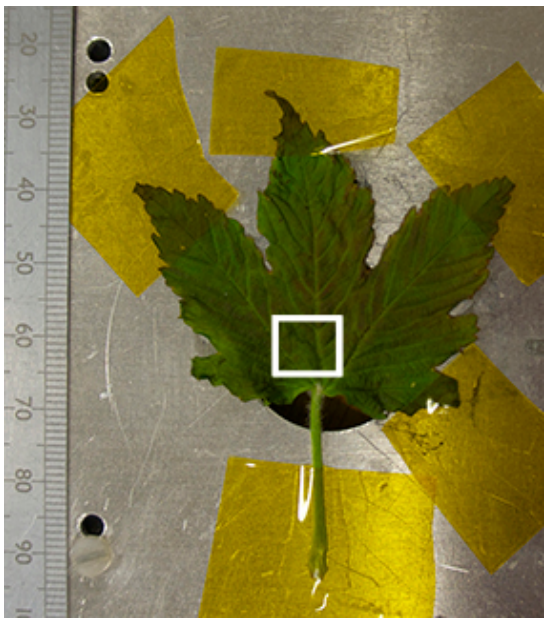

S1.3. Fossil accession numbers.

BHI prefix refers to the Black Hills Institute Museum, part of the Black Hills Institute of Geological Research (Hill City, South Dakota), confirmed by an independent expert engaged by the Royal Society as a suitable repository for palaeontological material as set out within the rules of the Society of Vertebrate Palaeontology (SVP). Accession numbers with an MGSF prefix refer to the permanent palaeontological collection kept by the University of Manchester School of Earth, Atmospheric, and Environmental Sciences. This collection also satisfies the repository rules of the SVP.

S1.4. BHI-7032

This block contains two leaves, the smaller of which (~ 2 cm x 2 cm) is identified as *Platanus wyomingensis*, the larger leaf in tentatively identified as *Cedrelospermum nervosum* (Manchester, 1989) . Parachute Creek Member of the Green River Formation (near Douglas Pass, Colorado).

S1.5. BHI-3113

Fossil leaf (*P. wyomingensis*), Bonanza locality, Utah. near the town of Bonanza, Uinta County, northeast Utah, Uinta Basin.

S1.6. BHI-045A

Fossil reptile (Squamata: Reptilia tent.), and fossil leaf (*P. wyomingensis*). Ray Dome locality near Douglas Pass, Colorado, Upper Parachute Creek Member, Green River Formation.

S1.7. MGSF312

Macginitiea wyomingensis, Bonanza locality, Utah. Py-GC/MS. Large size and poorer structural preservation made this more suitable for destructive analysis than BHI-7032.

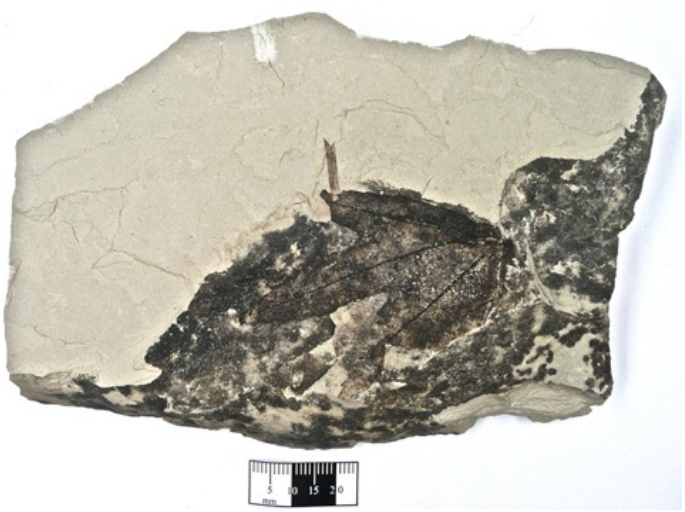

S1.8. MGSF313

Zelkova nervosa, Douglas Pass locality, Colorado.

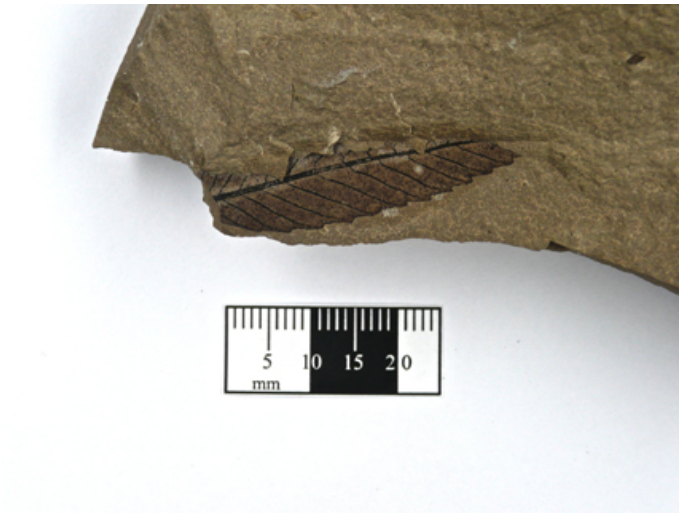

S1.9. BHI-3100

Populus wilmattae (Poplar), Bonanza locality, Utah.

S2. Geological Setting

The Green River Formation of Wyoming, Colorado and Utah (USA) spans much of the early and middle Eocene (~55-40 Mya) and was deposited in two intermontane basins: the Greater Green River Basin of Wyoming and the Uinta-Piceance Creek Basin of Colorado and Utah (Smith et al., 2008; Bradley, 1964; Roehler, 1992; Dickinson et al., 1988; Dyni, 2006). The formation represents a fluctuating lacustrine setting (Smith et al., 2008; Bradley, 1964; Roehler, 1992; Dickinson et al., 1988). Volcanism occurred over wide areas of the northwestern USA and introduced volcaniclastic sediment to the Green River Formation basins (Smith et al., 2008; Surdam et al., 1980; Fritz and Harrison, 1985). There were three lakes that now yield abundant fossils: Fossil Lake and Lake Gosiute of the Greater Green River basin, and Lake Uinta of the Uinta- Piceance Creek basin (Grande, 1984; Smith et al., 2008). Both the fossil fauna and flora indicate a warm temperate to subtropical environment (Grande, 1984; Roehler, 1992; Dyni, 2006). The Green River Formation is best known for its abundant oil shale (Grande, 1984; Tissot & Welte) and sodium carbonate resources (Dyni, 2006). The matrices of the fossils generally consist of extremely fine-grained, finely laminated shale/mudstone from the Upper Parachute Creek Member from which the majority of fossils in the Uinta and Piceance Creek Basins are found.

S3. Supplementary Methods: Experimental Details

Sample handling and storage

All fossil samples are isolated in their own packaging. Surgical gloves were used in all handling. For FTIR analysis the ATR crystal was cleansed with laboratory wipes and deionised water after each sample change. No contamination of the ATR crystal was observed at any time in any of the analyses presented here.

X-ray Diffraction

Experiment parameters are outlined in Edwards et al 2011.

Pyrolysis-Gas Chromatography/Mass Spectrometry

BHI-7032 and BHI-3113 are too scientifically valuable to be subjected to destructive analysis, therefore another comparable but less well preserved Green River specimen from the same family (Wolfe & Wehr, 1987) was subjected to destructive analysis [*Macginitiea wyomingensis* - MGSF312].

M. wyomingensis leaf material and its surrounding sedimentary matrix were collected using sterile scalpels and 2 µg analysed by normal flash and TMAH (tetramethylammonium hydroxide) assisted Py-GC/MS. Normal flash pyrolysis samples underwent no additional treatment, samples subjected to TMAH assisted Py-GC/MS were prepared by soaking the sample in 5 µl of TMAH for 5 mins. Samples were analysed following the protocol employed in Edwards et al., 2011. For normal flash pyrolysis a scanning range of *m/z* 45-650 was used, and the oven was programmed from 40°C (held for 4 mins) to 320°C at 5°C min^{-1} and held at this temperature for 15 min. For TMAH assisted Py-GC/MS a scanning range of *m/z* 60-650 was used, and the oven programmed from 40°C (held for 4 mins) to 320°C at 5°C min^{-1} and held at this temperature for 5 min. Compound identification performed by comparison with previously published literature.

References

Bradley, W.H. 1964 The geology of the Green River Formation and associated Eocene rocks in southwestern Wyoming and adjacent parts of Colorado and Utah. *U.S. Geological Survey Professional Paper* **496-A**, 86.

Dickinson, W.R. et al., 1988 Paleogeographic and Paleotectonic Setting of Laramide Sedimentary Basins in the Central Rocky-Mountain Region. *Geological Society of America Bulletin* **100**, 1023.

Dyni, J.R. 2006 Geology and resources of some world oil-shale deposits. *U.S. Geological Survey Scientific Investigations Report* **2005-5294**, 42.

Edwards et al., 2011 Infrared Mapping Resolves Soft-Tissue Preservation in 50 Million Year Old Reptile Skin. *Proceedings of the Royal Society B: Biological Sciences* **278**:3209-3218.

Fritz, W.J., and Harrison, S. 1985 in *Cenozoic paleogeography of the west central United States: Rocky Mountain Section* R. M. Flores, S. S. Kaplan, Eds. (Society of Economic Paleontologists and Mineralogists, Rocky Mountain Paleogeography Symposium), vol. 3, pp. 282-402.

Grande, L. 1984 *Paleontology of the Green River Formation, with a review of the Fish Fauna.* (The Geological Survey of Wyoming, ed. 2nd).

Manchester, S. R., 1989. Attached Reproductive and Vegetative Remains of the Extinct American- European Genus Cedrelospermum (Ulmaceae) from the Early Tertiary of Utah and Colorado. *American Journal of Botany* **76**, 256-276.

Roehler, H.W. (1992) Correlation, compostion, areal distribution, and thickness of Eocene stratigraphic units, greater Green River basin, Wyoming, Utah, and Colorado. *U.S. Geological Survey Professional Paper* **1506-E**, 49.

Smith, M.E., Carroll, A.R., and Singer, B.S. 2008 Synoptic reconstruction of a major ancient lake system: Eocene Green River Formation, western United States. *Geological Society of America Bulletin* **120**, 54.

Surdam, R.C., and Stanley, K.O. 1980 Effects of changes in drainage-basin boundaries on sedimentation in Eocene Lakes Gosiute and Uinta of Wyoming, Utah, and Colorado. *Geology,* 8, 135 - 139.

Tissot, B. & Welte, D. H. 1984 *Petroleum Formation and Occurence,* Berlin, Springer.

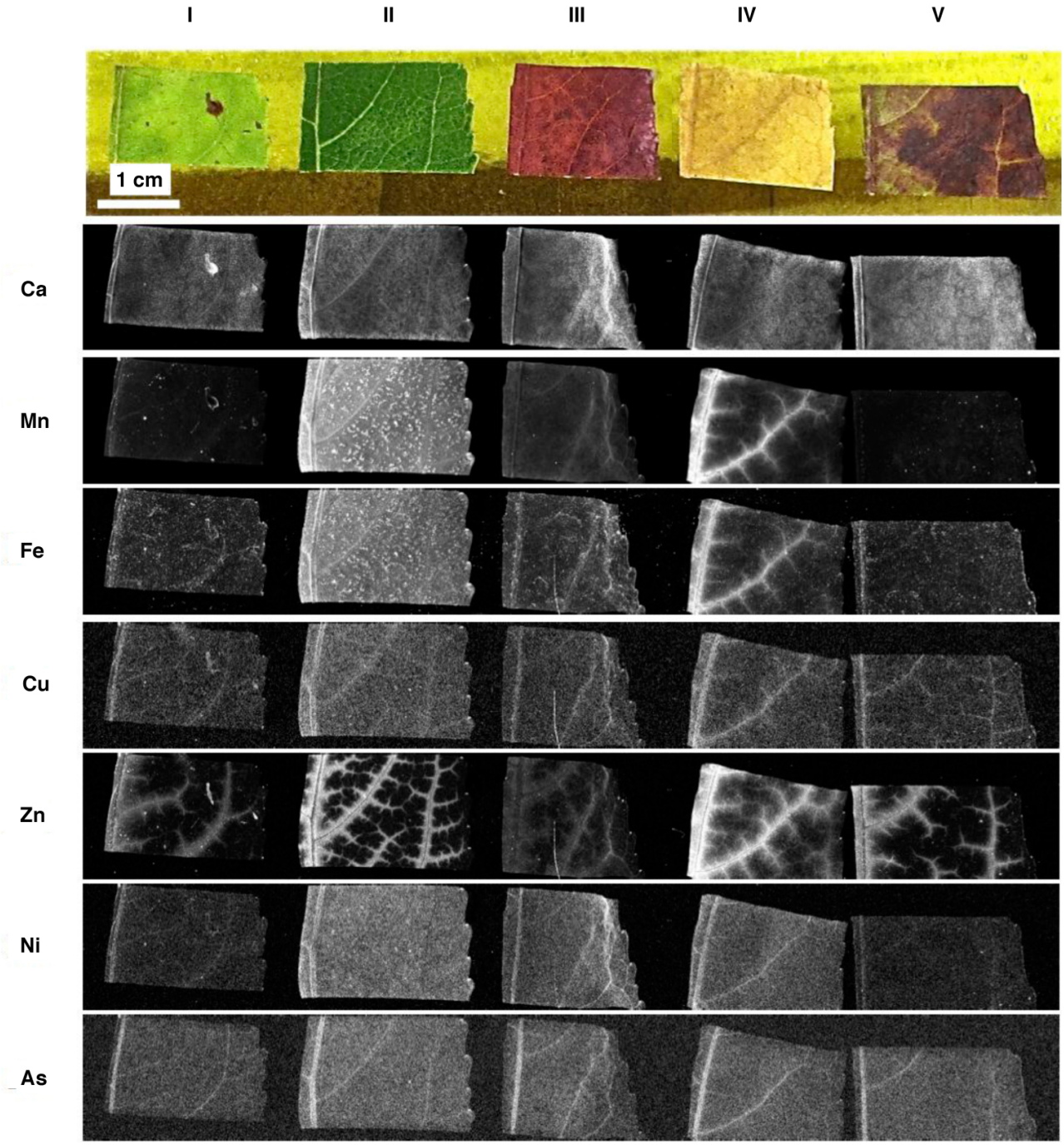

Figure S1. SRS-XRF maps of extant leaf material *Liquidambar styraciflua* at varying degrees of senescence. Interestingly Mn, which is the metal cofactor in photosystem II, is broadly distributed within the green leaf (column II) as would be expected for actively photosynthesizing tissue, however in the yellow leaf Mn has been withdrawn and is concentrated within the veins (column IV).

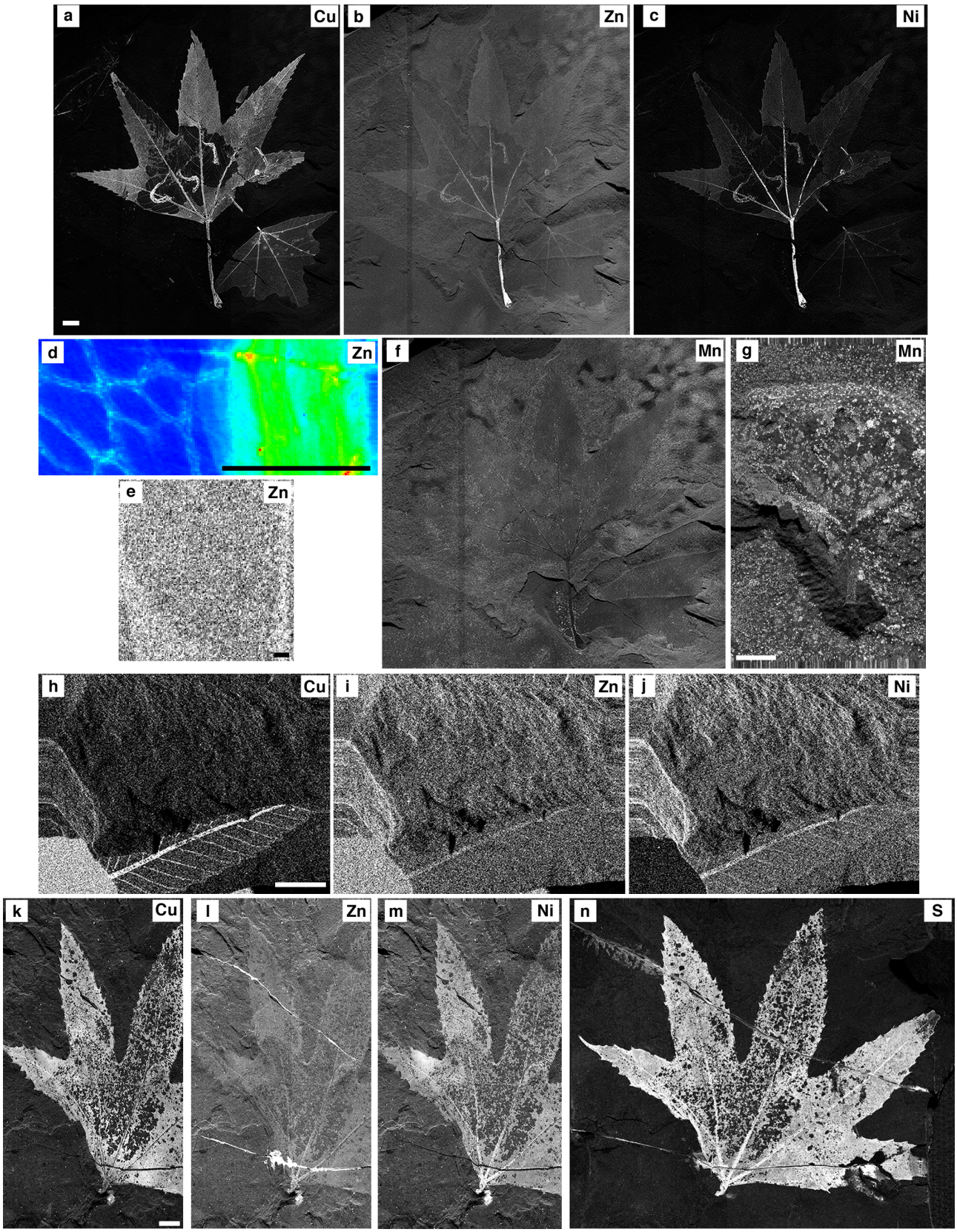

Figure S2. Additional SRS-XRF maps of fossil and extant leaves. (a-c) *P. wyomingensis* (BHI-3113), Cu, Zn, Ni respectively; (d) extant *A. pseudoplatanus,* Zn; (e) *P. wyomingensis* (BHI-3113) at high magnification, Zn; (f) *P. wyomingensis* (BHI-3113), Mn; (g) *P. wyomingensis* (BHI-7032), Mn; (h-j) *Z. nervosa* (MGSF313), Cu, Zn, Ni respectively; (k-n) *P. wyomingensis* (BHI-045A), Cu, Zn, Ni, S respectively. Scale bars: (a,h,k) 1 cm; (d,e) 1 mm; (g) 5 mm.

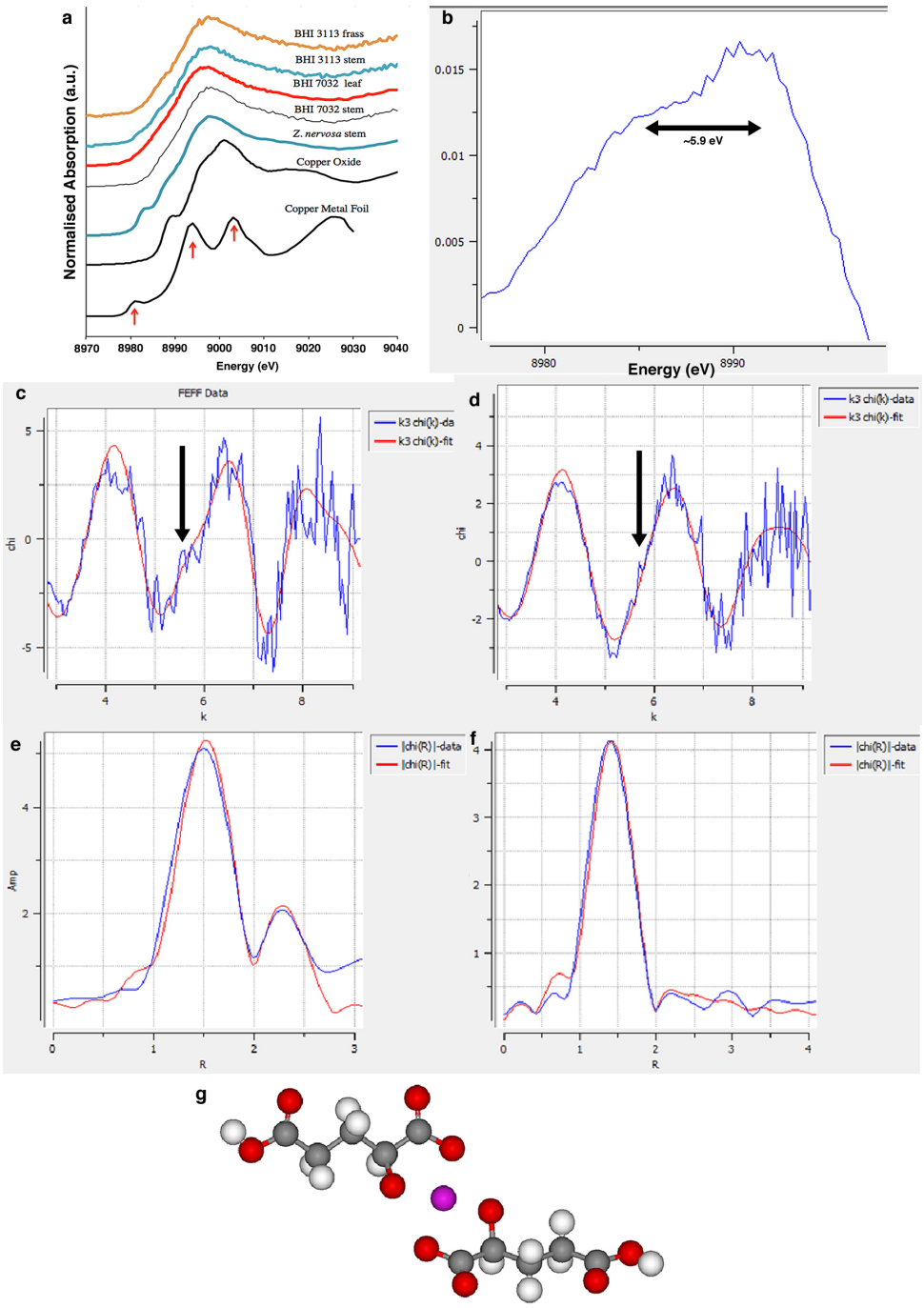

Figure S3. X-ray absorption analyses of Cu. (a) XANES spectra at the Cu Kα edge for Cu metal foil and Cu oxide standards, *P. wyomingensis* [BHI-7032 and BHI-3113, acquired at SSRL 6-2] stem, leaf and frass tubes, and *Z. nervosa* (MGSF313, acquired at DLS I18). Arrows on the Cu oxide spectrum indicate spectral features that are weak or absent on the fossils. (b) First derivative of the Cu K-edge XANES spectrum from BHI-7032 *P. wyomingensis* leaf. Bifurcated peak results from distortion of the coordination polyhedron and indicates that the axial oxygens are approximately 2.42 angstroms radially distant from the central Cu absorber. EXAFS k^3 χ(k) spectra at the Cu K-edge for (c) *P. wyomingensis* [BHI-7032, acquired at SSRL 6-2] and (d) *Z. nervosa* (MGSF313, acquired at DLS I18). EXAFS Cu K-edge radial distribution function (RDF) for (e) BHI-7032 *P. wyomingensis* showing non-phase shift corrected data (blue) and fit (red). The signal to noise ratio is relatively high, however the fit does closely reproduce the data. To compare the data above to ED Table 2, a phase shift correction of approximately 0.465 Å to the radial distances shown above should be applied. The first peak is due to the square planar first shell of equatorial oxygens, while both the Cu-C and Cu-O (ax) shells contribute to the smaller second peak. (f) *Z. nervosa* (MGSF313) RDF (symbols same as previous) with third shell carbon included (as for malate-type ligand). Reduced chi-square improves from 2.74 to 0.67 with inclusion of carbon shell. Black arrows highlight spectral feature consistent with malate type coordination for Cu, clearly present on (c) and present but weak on (d). (g) Proposed model for

Cu within the fossil leaf material. Cu is most likely coordinated to two malate molecules, forming two five-membered rings. Inner shell oxygen and second shell carbon distances are all to scale and based on the EXAFS results of BHI-7032 presented in ED Table 2 (element colour code: red = O, white = H, grey = C, magenta = Cu).

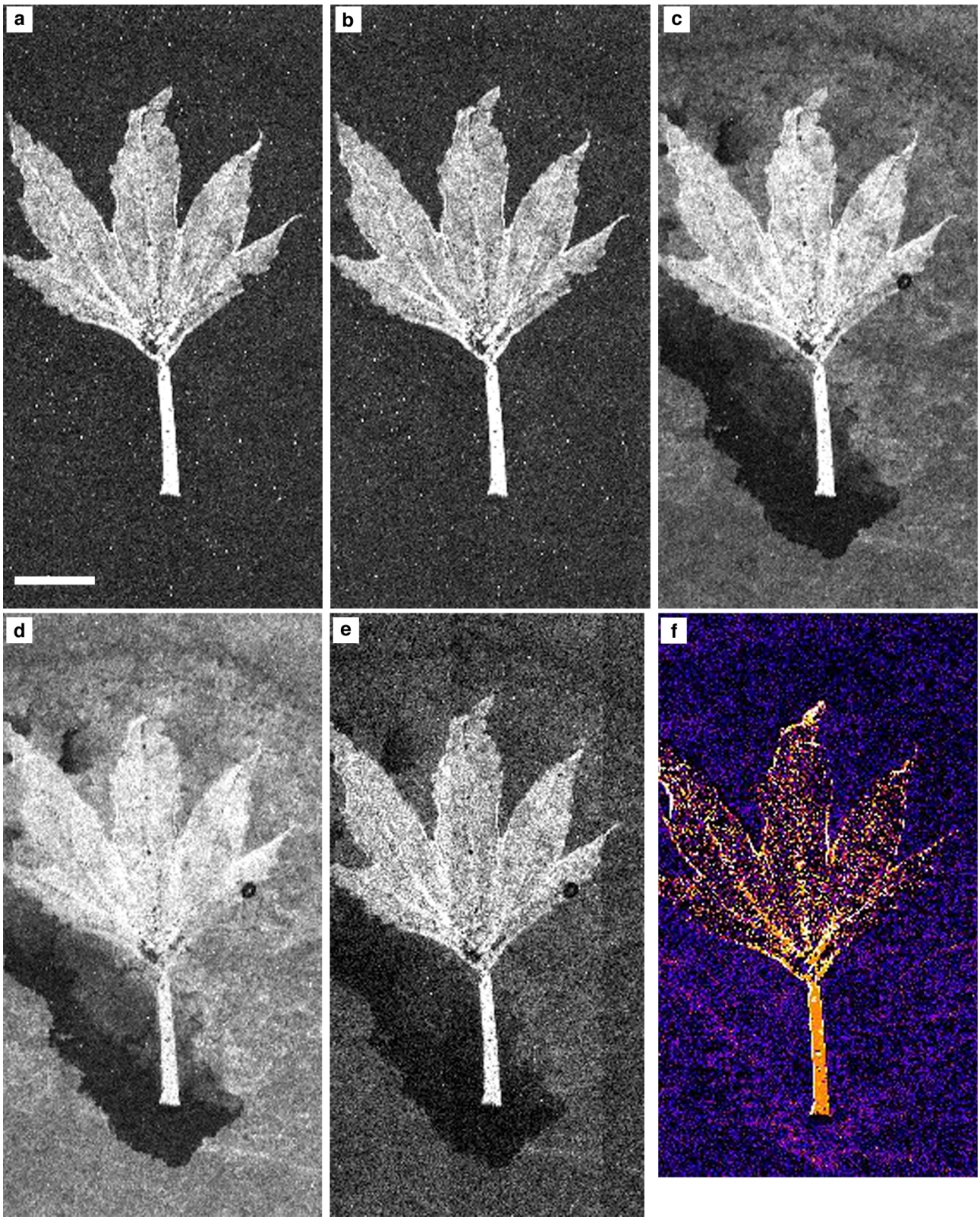

Figure S4. SRS-XRF maps of the sulfur oxidation states identified within *P. wyomingensis* (BHI-7032) (a) thiol, 2472.9 eV, (b) methionine sulfoxide, 2474.6 eV (c) sulfonate, 2480.4 eV (d) sulfate, 2481.4 eV, (e) total sulfur, 3150 eV. (f) Thiol/copper cross-correlation map, bright areas indicate positive correlation. Scale bar = 5 mm.

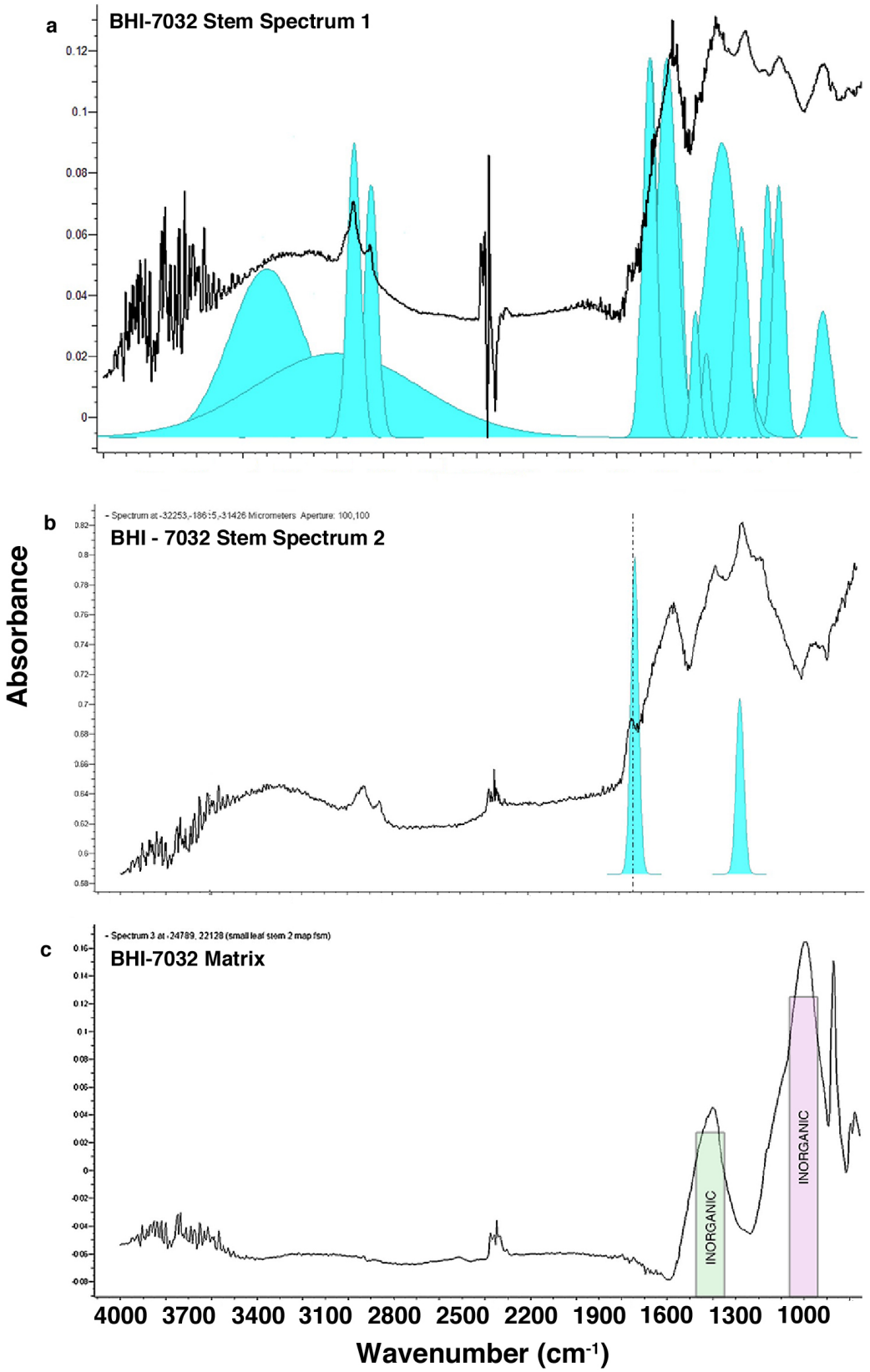

Figure S5. FTIR spectra of BHI-7032 with absorption band assignments for selected peaks. (a) Spectrum taken from the stem of *P. wyomingensis*. Vibrations corresponding to C-H (alkanes), C=O, O-H, C-O (carboxylates) and CNH (amide) marked in blue. (see ED Table 3 for full band assignments). (b) Additional FTIR spectrum from the stem of BHI-7032 *P. wyomingensis* demonstrating the occurrence of an absorption peak at 1740 cm^{-1} (blue areas) most likely the C=O of an ester. (c) Sedimentary matrix: calcite peaks (green box) and silicate stretch region (grey box) as confirmed by XRD analysis; no organic peaks are easily distinguishable.

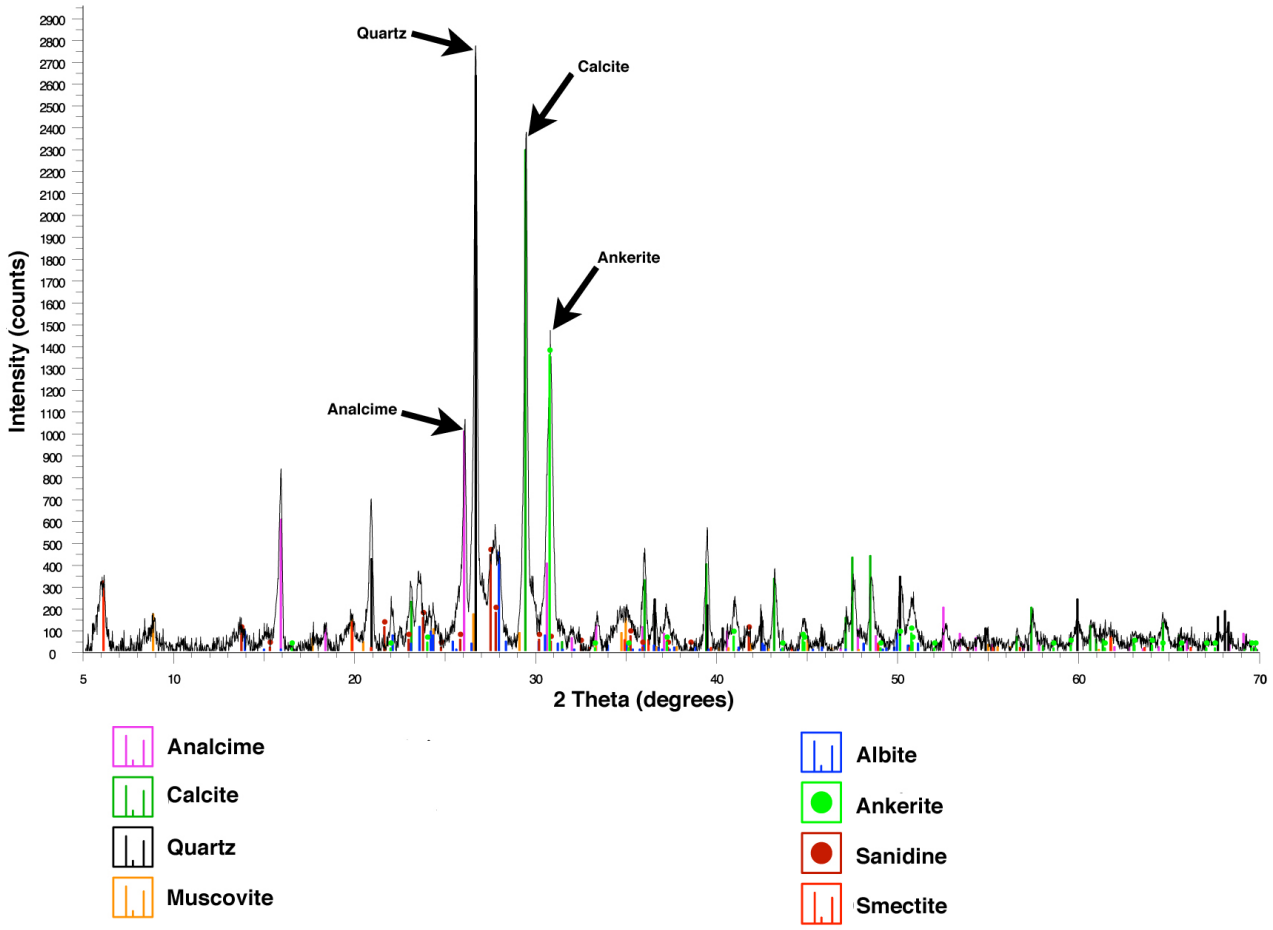

Figure S6. X-Ray Diffraction analysis of powdered bulk sedimentary matrix of specimen BHI-7032. Quartz, calcite, and ankerite are the dominant silicate and carbonate minerals present. Analcime, albite, and small amounts of smectite and muscovite are also identified as silicate minerals present in the sedimentary matrix. Diffraction peaks corresponding to reference patterns are colour coded and defined in the key.

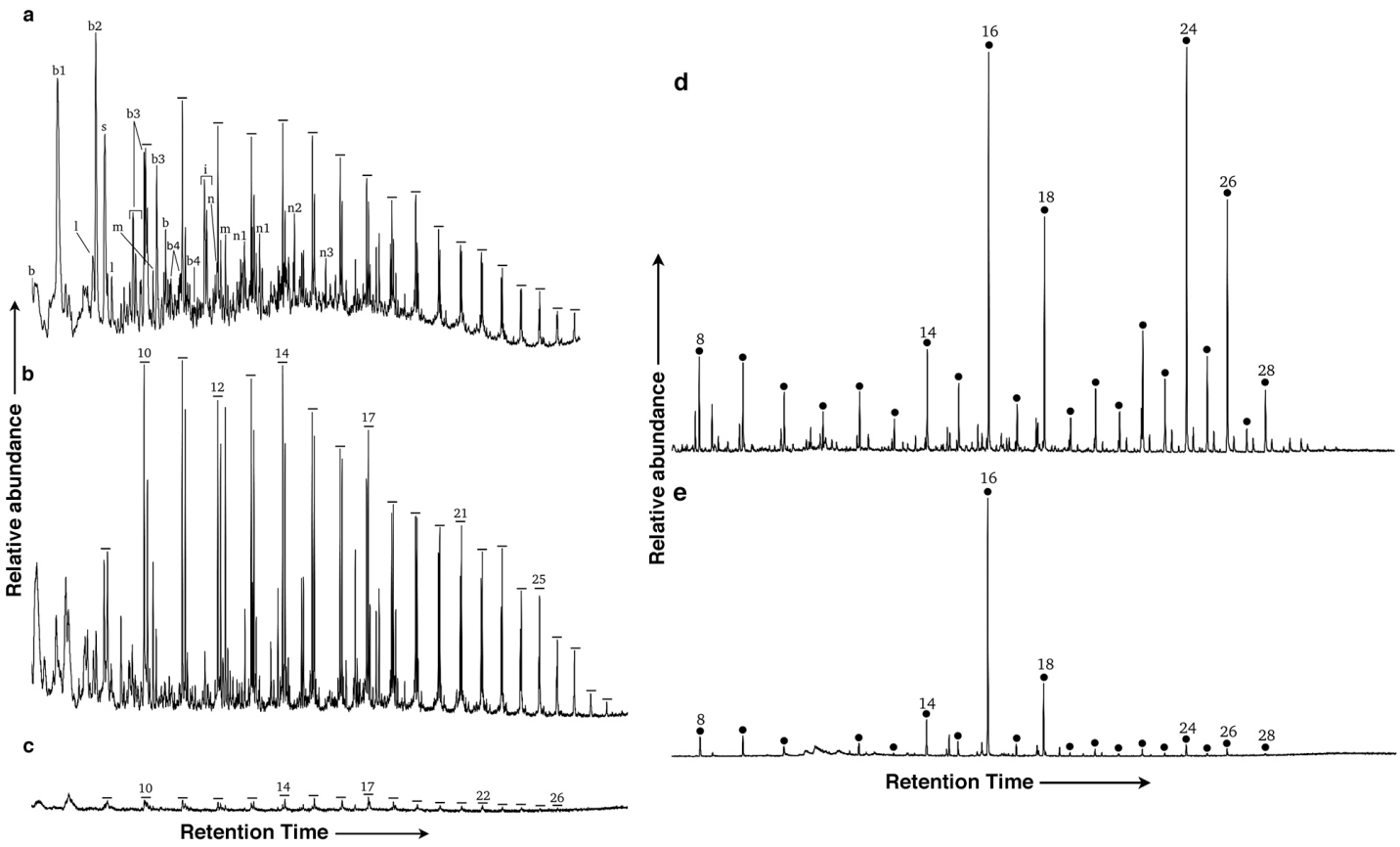

Figure S7. (a) Partial Py-GC/MS total ion chromatogram of bulk fossil leaf sample. (b) *m/z* 55+57 mass chromatograms showing the distribution of *n*-alkane/alkene moieties of fossil leaf (MGSF312) and (c) sedimentary matrix. (b) and (c) to scale, (a) independently scaled. Numbers indicate carbon chain length. -, *n*-alkane/alkene doublet; b, benzene; b1, methylbenzene; b2, dimethylbenzene; b3, trimethylbenzene; b4, tetramethyl benzene; l, 2-methylphenol (lignin moiety); s, styrene; n, naphthalene; n1, napthalenemethyl; i, indenemethyl; m, methylated alkanes. TMAH assisted partial Py-GC/MS *m/z* 74 mass chromatograms of MGS312 (d) fossil leaf and (e) sedimentary matrix, showing the distribution of generated fatty acid (measured as methyl esters). The fossil is dominated by fatty acids ranging in carbon number from C_8 to C_{28} with an even over odd predominance and maxima at C_{16} and C_{24}. The fatty acid distribution in the matrix is clearly different from the fossil leaf, with analogues ranging in chain length from C_8 to C_{28}, a less significant even over odd predominance, and maxima at C_{16} and C_{18}. All chromatograms are to scale, numbers indicate carbon chain length and dashes and closed circles indicate *n*-alkane/alkene doublets and fatty acids, respectively.

Table S1. Synchrotron XRF (ppmW) and VP-FEG-SEM[a] (wt. %) quantitative point analyses[b]

	L. styraciflua	*A. pseudoplatanus*	BHI-7032			BHI-3113					BHI-3100			MGSF313		
	n = 10	Stem	Stem	Lobe	Matrix	Stem	Vein	Lobe	Frass	Matrix	Stem Base	Stem Top	Matrix	Vein	Leaf	Matrix
Mn	6,938	1,404	458	128	731	0	365	921	696	445	91	71	53	164	230	226
Fe	189	1218	†	†	11,700	†	†	†	†	23,430	†	†	11,260	†	†	13,600
Ni	56	111	341	56	67	3786	850	219	653	28	90	42	63	52	80	56
Cu	6	470	1284	178	25	886	1458	884	2589	37	336	63	31	73	102	23
Zn	209	2257	74	51	58	1475	136	84	114	80	43	41	58	39	47	55
Ca	2,366*	8348	†	†	66,820	†	†	†	†	149, 955	†	†	158,400	†	†	123,000
Si	6,644	-	18,850	25,370	134,400	15,730	30,880	47,410	48,200	102,500	-	-	-	5462	-	-
S	153*	-	1,893	2,214	1,998	8457	11,410	9552	13,480	638	-	-	-	143	-	-
Ca (SEM)	-	-	5.59%	6.53%	11.29%	-	-	-	-	-	-	-	-	-	7.6%‡	10.00%
S (SEM)	-	-	0.57%	0.50%	0.44%	-	-	-	-	-	-	-	-	-	2.1%‡	0%
C (SEM)	-	-	52.29%	40.10%	20.57%	-	-	-	-	-	-	-	-	-	30.4%‡	11.90%

* n = 5 ‡ n = 3 † cannot be resolved BDL = below detection limits - = data not obtained

[a]*VP-FEG-SEM* was completed using a Zeiss Supra40 instrument at the DRIAM Analytical Service, Dalton Research Institute, Manchester Metropolitan University. All samples were analyzed without any chemical or physical alteration to their surface. Standard clean laboratory sampling handling protocols were used throughout. Point analyses of elements present were acquired in variable pressure mode (~0.5 torr) using standardless energy dispersive spectroscopy (EDS, Oxford Instruments) at 15 kV, take-off angle of 35.5°, and a working distance of 15 mm. Spectra collected were fitted and elements quantified using proprietary ZAF-corrected software. Counting times in excess of 100 live seconds were performed to maximise the signal-to-noise ratio of the spectra.

[b]For those elements that are dominantly concentrated within the organic residues (including Cu, Zn and Ni) the concentrations given above are estimated to be accurate to +/- 10% relative. Due to the fact that the thin fossil films are low in atomic weight and that there are inherently high levels of Ca and Fe in the mineral matrices for these samples, fluorescence from the underlying matrix is detected through the thin films. This means that it is difficult to deconvolve concentrations of Ca and Fe in the organic fossil thin films from that of the matrices. These problems also affect SEM analyses. In particular, sulfur in the BHI-7032 matrix is also relatively high, and so the ability to map different sulfur oxidation states by tuning the energy of the incident radiation is a huge advantage of synchrotron analysis.

Table S2. EXAFS fitting details.

	n	R(Å)	σ^2	ΔE	χ^2_ν	So2
Copper Oxide						
Cu-O (eq)	2.9	1.949	0.002			
Cu-O (ax)	3.2	2.879	0.001			
Cu-Cu	0.8	3.454	0.001			
Cu-Cu	6.2	5.282	0.009	-0.43	47.66	0.79
Fossil Leaf (BHI-7032, *P. wyomingensis*)						
Cu-O (eq)	3.9	1.960	0.0056			
Cu-O (ax)	1.7	2.423	0.005*			
Cu-C	4.9	2.872	0.005*	0.067	5.08	0.66
Fossil Leaf (MGSF313, *Z. nervosa*)						
Cu-O (eq)	3.9**	1.91	0.0049			
Cu-O (ax)	2.1	2.537	0.0023			
Cu-C	1.5	2.874	0.0015	-6.81	0.67	0.133**

* fixed parameter
** poor signal to noise resulted in low amplitude EXAFS oscillations; in order to produce realistic coordination numbers So2 was set to give n1 = 3.9 to match the BHI7032 data. After fixing the correlated parameters n1 and So2 at the values shown, all other variable values were obtained from unconstrained iterative fits.

Table S3. FTIR absorption band assignments.

	Functional Group	Bond	Wavenumber Range (cm-1)	Mode of Vibration
BHI-7032 Stem	Alkane	CH	2936-2916	antisymmetric stretch
		CH	2863-2843	symmetric stretch
		CH	1485-1445	deformation
	Carbo-acid	C=O	1610-1560	stretch
		C=O	1400-1300	stretch
		C=O	1670-1650	stretch
		C-O	1320-1211	stretch
	Ester	C=O	1740-1720	stretch
	Alcohol	OH	3400-3200	stretch
		OH	1410-1310	deformation
		C-O	1210-1100	stretch
	Amide	N-H	3320-3270	stretch
		C=O	1680-1630	stretch
		CNH	1570-1515	combination
		CNH	1305-1200	combination
	Nitro	N-O	1560-1500	asymmetric stretch
		N-O	1390-1330	symmetric stretch
BHI-7032 Matrix	Silica	Si-O	1190-940	bridging stretch
		Si-O	1080	apical stretch
		Si-OH	3600-3200	stretch
	Calcite	C-O	1430	stretch
		C-O	873	stretch